REEXAMINATION OF THERMAL CYCLING RELIABILITY OF BGA COMPONENTS WITH SNAGCU AND SNPB SOLDER JOINTS ON DIFFERENT BOARD DESIGNS

Sinan Su[1], Francy Akkara[1], Thomas Sanders[2], Jiawei Zhang[3], John Evans[1], Gregory Harris[1]
[1]Department of Industrial and Systems Engineering
[2]NASA Jet Propulsion Lab
[3]Broadcom Limited
AL, USA
gah0015@auburn.edu

ABSTRACT
In this paper, a direct comparison was conducted between SnPb and lead-free solder joints focused on long-term thermal cycling reliability after being exposed to high-temperature aging for a long period of time using two test vehicle designs. Ball Grid Array (BGA) packages with SAC305 (Sn-3%Ag-0.5%Cu) and eutectic SnPb (63%Sn-37%Pb) were compared in this research. After the test, IMC thickness and failure modes of BGA components on the different test vehicles were investigated. The results from the post-test examination were analyzed to explain certain unexpected outcomes of the two test vehicle designs when comparing the reliability results among the two programs of tests. The results showed that for the TC1 test vehicle, SAC305 solder joints show better reliability than the SnPb solder joints; while the reliability of the SnPb solder joints outperformed the SAC305 solder joints after 6 months of high-temperature aging for the TV7 test vehicle. Meanwhile, even on the same test vehicle, the failure modes varied between components with SAC305 and SnPb solder joints.

INTRODUCTION
Tin-lead (SnPb) solders have been used extensively for various purposes for thousands of years. Historically, the choice of solder material for electronic assemblies was SnPb because of a variety of advantages SnPb solder materials held over other solder materials in electronic applications. Unfortunately, despite its many advantages, eutectic SnPb solder has been essentially eliminated in the past two decades to comply with the government legislations due to the toxicity concern of the lead, and the transitioning of the electronics industry to lead-free processes [1-5].

Harsh environment industries, such as aerospace, automotive, and military have enjoyed exemption from this industry conversion for more than a decade. Even though most of these exemptions are expiring, and the industries have been using the commercial-off-the-shelf (COTS) products which are regulated by the legislation, the main concern towards lead-free conversion lies in the fact that lead-free solder materials do not meet the reliability requirements for the products they are used in compared to the tin-lead solder materials previously used in those applications. The properties of SnPb have been extensively studied and used for a long time. But, the end users who have enjoyed the benefit of the exemptions have tended to continue the usage of SnPb until the substitutions (e.g. lead-free solders) can be proven to have the overall reliability equal or better than the eutectic SnPb solders [6, 7].

In ball grid array (BGA) applications solder joints play a critical role to the reliability of the assembly, given that the solder joints are the only connection between the package and board and a single solder joint failure will cause the malfunction of the final assembly [8-15]. Because of the restrictions from WEEE and RoHS, most of the commercially available solder joints of BGA are lead-free, and SAC305 (Sn-3%Ag-0.5%Cu) has become the most popular market choice [16-20]. However, eutectic SnPb provides many advantageous properties over lead-free, such as single transition temperature, low melting point, low cost, and good wetting ability etc. [6, 21, 22]. Beyond that, SnPb solder also provides adaptable mechanical, thermal, and electrical performance required in the modern electronic packaging applications. Given the eutectic SnPb solder undergoes a different and more limited microstructure evolution over time, the reduction in the loss of reliability and mechanical strength in the solder joint is less than the lead-free solder.

During the past decade, Auburn University has conducted the thermal cycling tests directed from industry and government partners with NSF's Center for Advanced Vehicle Electronics (CAVE). Three phases of tests were developed, and extensive results were published by generations of researchers on the thermal cycling reliability of various solder materials including SnPb and lead-free varieties [22-32]. However, some hidden insights come into light when the results from the different phases and tests are compared, rather than analyzing the data individually. Therefore, in this paper, the primary objective is to reexamine the long-term thermal reliability of SnAgCu and

SnPb solder joints of a certain BGA package on different board designs.

Experimental Designs

Test Vehicle Design

Package designs in Phase I (TV7) and II (TC1) programs were analyzed and are shown in Figures 1 and 2. For TV7 test vehicle, FR-406 glass epoxy materials were used as board substrate with a glass transition temperature (Tg) of 170°C. The dimension of the board is 100mm X 67mm with a board thickness of 1.574mm (4 Copper layers). The board finishes used for this test vehicle are immersion Silver (ImAg), immersion Tin (ImSn), electroless Nickel immersion Gold (ENIG), and electroless Niclel electroless Palladium immersion Gold (ENEPIG). The solder mask design (SMD) pads failed much faster than the non-solder mask designed pad (NSMD), therefore, all the TV7 project components included in this study were NSMD pads for better analysis of aging and thermal cycling effects. BGA with various footprints (5mm, 10mm, 15mm, 19mm) were analyzed. Three solder alloys including SAC305 (Sn-3%Ag-0.5%Cu), SAC105 (Sn-1%Ag-0.5%Cu), and SnPb (62%Sn-38%Pb) were used to attach the BGA packages.

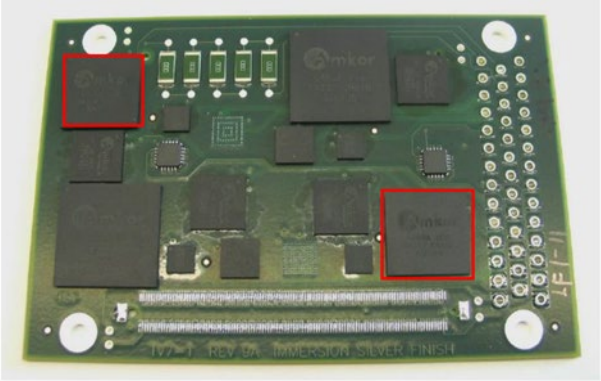

Fig. 1. Test vehicle design for TV7

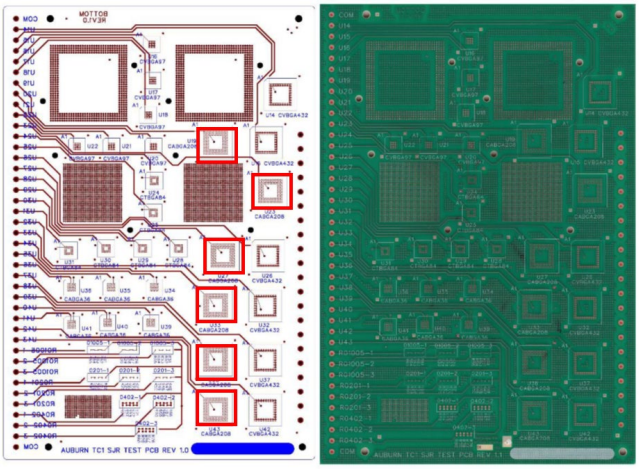

Fig. 2. Test vehicle design for TC1

Meanwhile, for the TC1 test vehicle design, the board dimension is 173mm X 254mm with a board thickness of 5mm (6 layers of Copper). The same FR-406 substrate materials were utilized in this project with a same glass transition temperature of 170°C. The components using NSMDs were used for the same reason as TV7 and the surface finish for all the testing boards was OSP. A larger range of packages were tested in the TC1 project, including PBGA with footprints varying from 5mm to 45mm. Most of the BGA components were plastic over-molded packages and two types of super-BGA (SBGA) packages (31mm, 45mm) were included in the study. Three types of solder pastes were used, including eutectic SnPb (62%Sn-38%Pb), SAC305 (Sn-3%Ag-0.5%Cu) and Innolot (SAC+Ni+Bi+Sb).

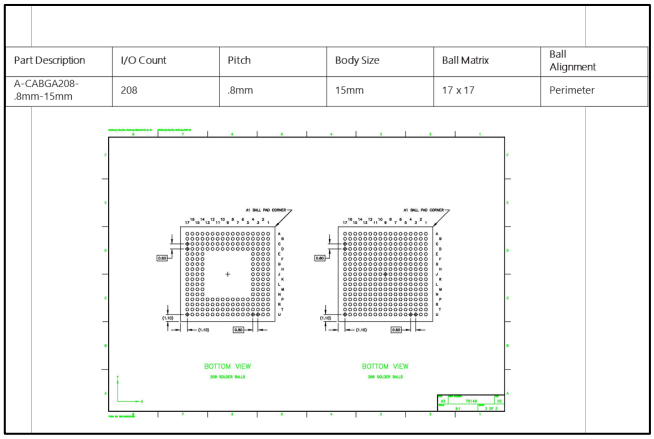

Fig. 3. 15mm BGA dimension

In this paper, the 15mm BGA with SAC305 and SnPb solder joints were analyzed and compared among the two test vehicles (red outlines in Figures 1 and 2) given they were included on both test vehicles with a moderate number of failures. Figure 3 shows the dimension of the 15mm BGA. The only difference for the 15mm BGA on TV7 and CT1 is that TV7 selected CTBGA208 and TC1 selected CABGA208, where the standout for CTBGA208 is 0.3mm smaller than CABGA208. In this project, only partial results were compared among the enormous data and a detail test vehicle comparison was shown in Table 1.

Table 1. Test vehicle comparisons between TV7 and TC1

	TV7	CT1
Board Thickness	1.57mm	5mm
Board Materials	FR-406	FR-406
Surface Finish	ImAg	OSP
Pad Design	NSMD	NSMD
Package Type	CTBGA208	CTBGA208
Solder Sphere Materials	SAC305, SnPb	SAC305, SnPb
Solder Paste Materials	SAC305, SnPb	SAC305, SnPb

Test Vehicle Assembly & Test Plan

TV7 and TC1 test vehicles were assembled following the similar steps, where solder pastes were printed on raw PCB with a stencil thickness around 4.5mil for the TV7 and 5mil for TV1. Then all the components were placed on top of the solder paste and the assemblies were sent to reflow. The

reflow profiles for the two test vehicles were created separately, where the TC1 reflow profile is more 'aggressive' in reaching the top temperature given the larger thermal mass of TC1 boards, and no soak zone was set. The thermal profiles were slightly modified when switching from the lead-free boards to the SnPb boards, given the differences in the melting temperature of each solder material. The reflow profiles are shown in Figures 4-5.

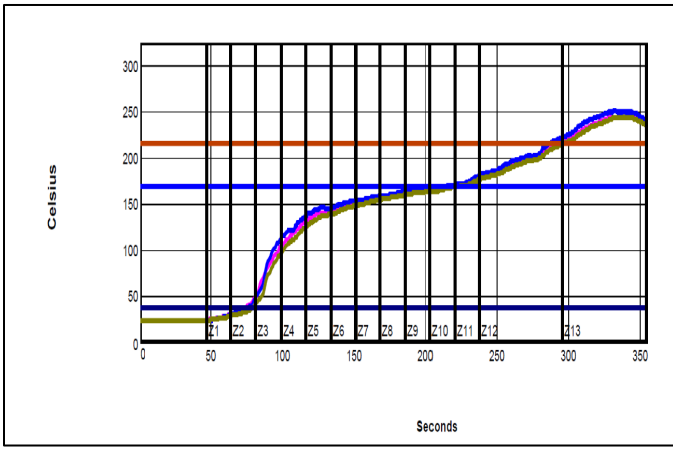

Fig. 4. Reflow profile for TV7

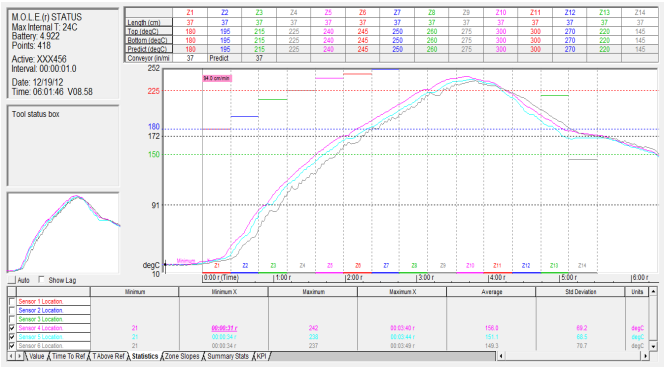

Fig.5. Reflow profile for TC1

Both TV7 and TC1 follow the JESD22-104B temperature cycling standard, condition 'G', where temperature range is from -40°C to +125°C, to assess the solder joint performance under a harsh environment. The highest temperature was set to be +125°C, given the JEDEC standard does not recommend test condition that exceed 125°C for SnPb solder materials. Different ramping temperatures were selected for each test, given the capability limits of the chambers used to carry out the tests and the thermal mass differences within the different test boards. The ramp time from the lower temperature extreme to the upper temperature extreme for TV7 is 15mins, while the ramp up for TC1 is 45mins. A detail test plan comparison is shown in Table 2.

Table 2. Test plan comparisons between 2 tests

	TV7	CT1
High Extreme	125°C	125°C
Low Extreme	-40°C	-40°C
Ramp time	15 Mins	45 Mins
Dwell Time	30 Mins	15 Mins
Total Time/Cycle	90 Mins	120 Mins
Aging Temperature	55°C	75°C
Aging Durations	0m, 6m, 12m, 24m	0m, 6m, 12m, 24m

Prior to thermal cycling the boards were exposed to different aging conditions. TC1 boards that were aged at 75°C from 0 month to 24 months were analyzed and compared with TV7 boards that were aged at 55°C from 0 month to 24 months.

Results and Discussions

Failure Data Analysis

A two-parameter Weibull distribution was utilized to characterize the fatigue life of the BGA after thermal cycling tests, expressed as in Equation 1:

$$R(t) = e^{-(\frac{t}{\theta})^{\beta}} \qquad (1)$$

where $R(t)$ is the reliability or the probability of survival, β is the shape parameter, θ is the scale parameter, and t is the number of cycles. The scale parameter is defined as the characteristic fatigue life, which is the number of cycles at 63.2% probability of failure. Mainly, two types of censoring methods were used to analyze the failure data: right censoring or interval censoring. Right censoring method was applied in the situation where all the components did not fail after the thermal cycling test, while the interval censoring method was applied to estimate the fatigue life when the cycle number is documented in an interval between two observations. Both the characteristic life (scale parameter) and B10 life (the point where 10% of the population of the test vehicle will fail) were calculated and compared. The parameter estimation method used in the Weibull analysis is maximal likely estimation (MLE).

Figures 6a through 6d present the Weibull distributions of the thermal cycling results for TV7 test vehicle after 0 months (m), 6 m, 12 m, and 24 m of aging at 55°C (triangle-SnPb; circle-SAC305). Without aging, both the B10 and the characteristic life for SAC305 were larger than SnPb, even though the difference was small. After 6 m of isothermal aging at 55°C, both the B10 and the characteristic life for SnPb solder outperformed the SAC305 solder. With the increase in aging period at elevated temperatures (12m, 24m), the fatigue life difference between both solder materials increased, while the reliability life for the SnPb solder continued to outperform.

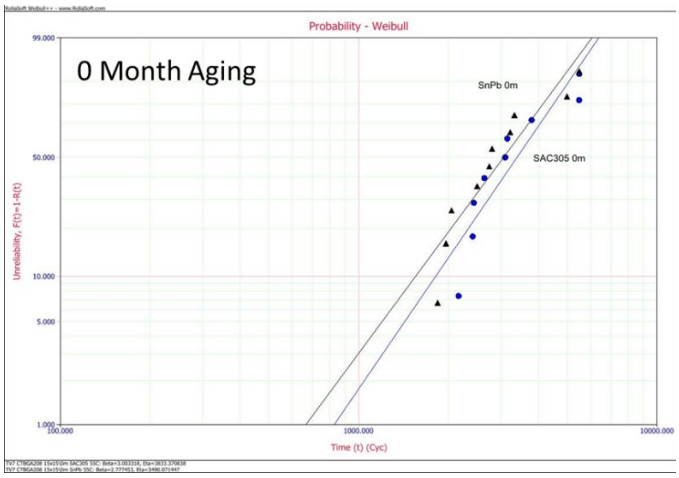

Fig. 6a. Thermal cycling results for SnPb vs. SAC305 at 0m aging for TV7

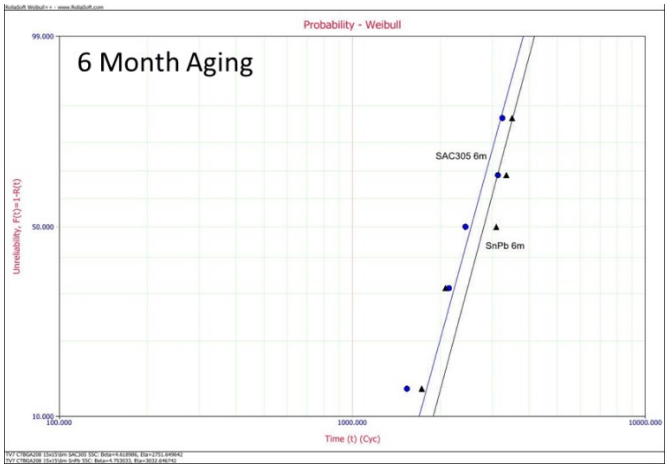

Fig. 6b. Thermal cycling results for SnPb vs. SAC305 after 6m aging for TV7

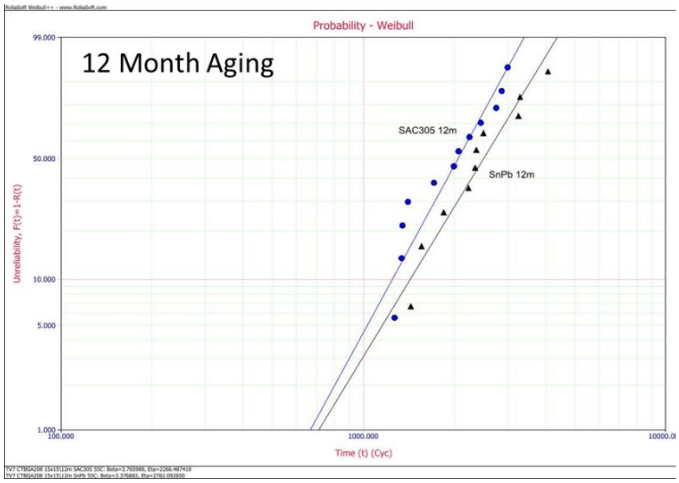

Fig. 6c. Thermal cycling results for SnPb vs. SAC305 after 12m aging for TV7

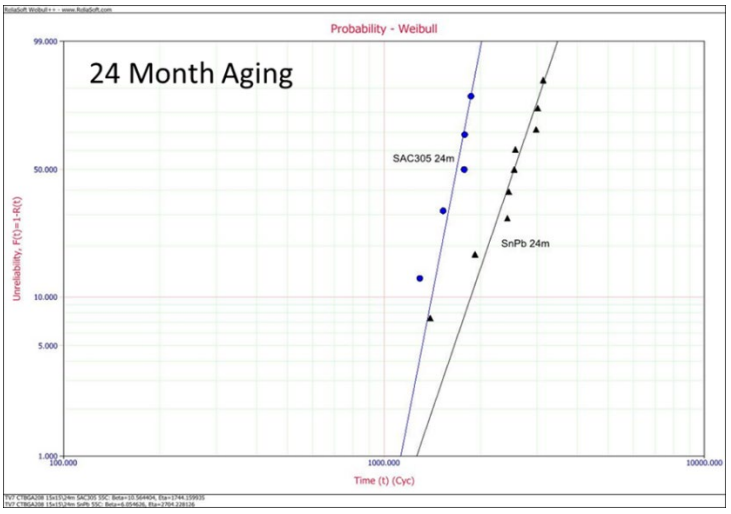

Fig. 6d. Thermal cycling results for SnPb vs. SAC305 after 24m aging for TV7

Figure 7 summarizes both the characteristic life and B10 life comparisons between the SAC305 and SnPb solder materials.

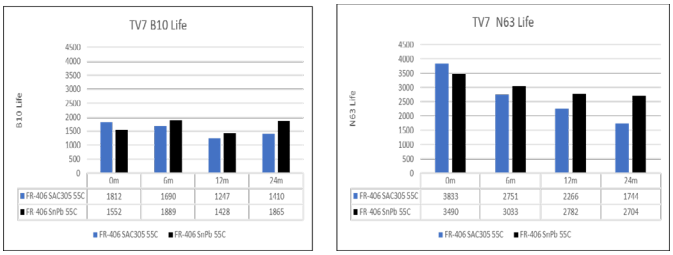

Fig. 7. B10 life and characteristic life comparisons between SAC305 and SnPb solder materials for TV7 with various aging conditions

BGA packages with the same footprints and pitch size (CABGA208) were analyzed in the TC1 project. Weibull distribution plots for the failure data after various aging durations were shown in Figures 8a-8d. The failure distributions associated with TC1 was different than the TV7. Mainly, SAC305 solder fatigue life was longer than SnPb for all the 4 aging durations (0m-24m), and SnPb solder material tended to fail in a narrower time frame. Figure 9 summarizes the fatigue life (N63 and B10 life) results for the TC1 test vehicle. In terms of N63 life, SAC305 solder outperformed the SnPb solder for all the aging durations. While in terms of B10 life, SnPb is slightly longer than SAC305 because of the larger shape parameter associated with the SnPb solder material.

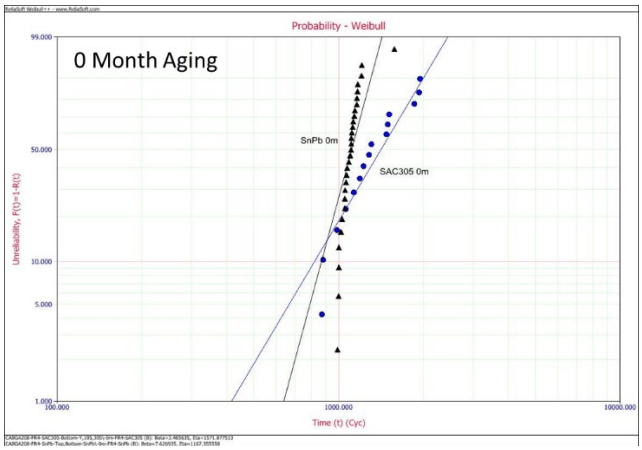

Fig. 8a. Thermal cycling results for SnPb vs. SAC305 at 0m aging for CT1

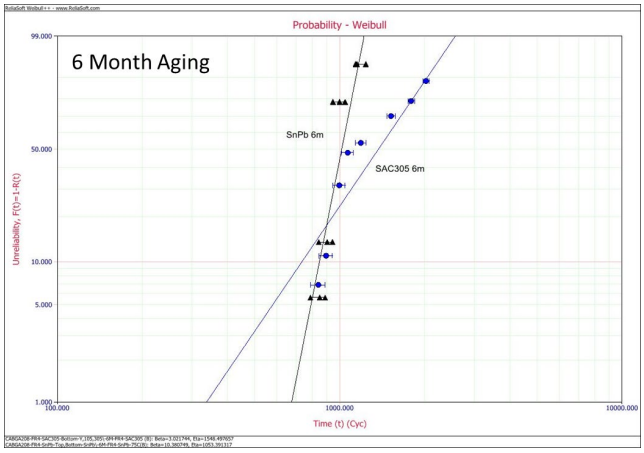

Fig. 8b. Thermal cycling results for SnPb vs. SAC305 after 6m aging for CT1

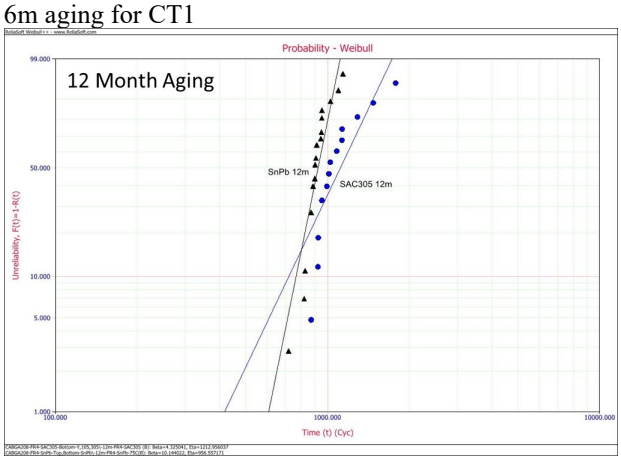

Fig. 8c. Thermal cycling results for SnPb vs. SAC305 after 12m aging for CT1

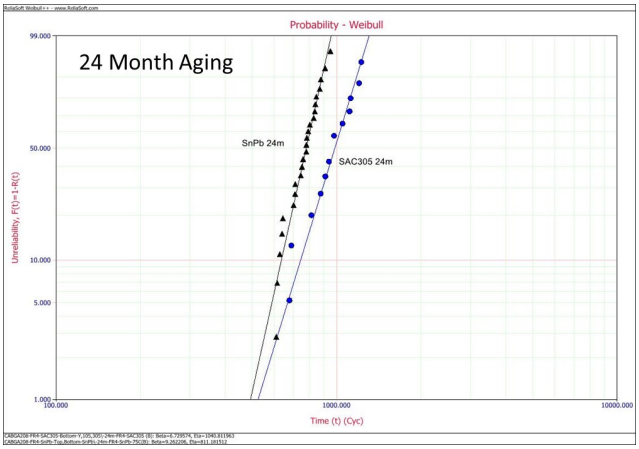

Fig. 8d. Thermal cycling results for SnPb vs. SAC305 after 24m aging for CT1

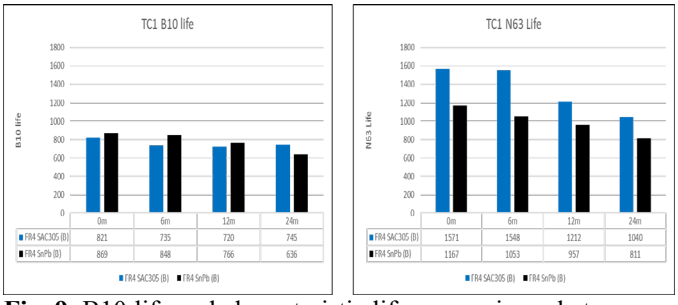

Fig. 9. B10 life and characteristic life comparisons between SAC305 and SnPb solder joints for Tc1 with various aging conditions

Shape parameters (β) of Weibull distributions for the two test vehicles (TC1 vs. TV7) are shown in Figure 10. For each aging condition, the shape parameters of TC1 are the two bars on the left and the TV7 shape parameters are the two bars on the right. One distinct observation from this figure is that the shape parameter of TC1 SnPb solder material is larger than the other three for 0m-12m aging, which indicates that the failing window was much faster than the rest. And the other three solder materials kept the similar pace in the failing process. Another observation from this figure is that most of the solder materials' shape parameter were increased after 2 years of elevated temperature aging, which might indicate that isothermal aging could not only deteriorate the reliability of BGA, but reduce the time interval for the complete failure of test vehicles.

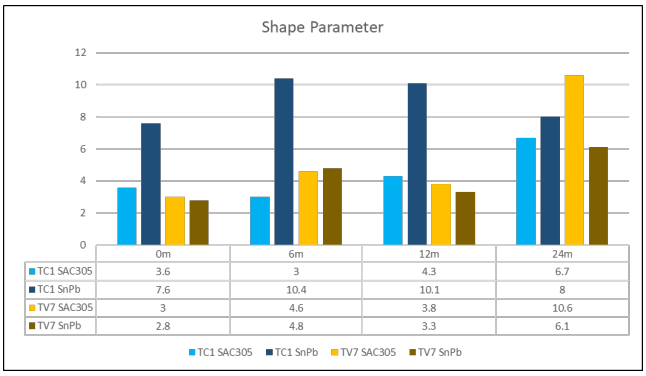

Fig. 10. Shape parameters comparisons between TV7 and TC1 with various aging conditions

Failure Modes Analysis

Intermetallic compounds (IMC) were studied to explain the different solder material behaviors within the TV7 test vehicle. When the molten solder contacts with the Cu pad, a layer of intermetallic compound is formed and servs as the bond between the solder joint and the Cu pad. The composition of the IMC depends on the solder joint composition, e.g. for the lead-free solder joints (Sn-Ag-Cu), the IMC mainly contained the needle shape Ag_3Sn and the scatter shape Cu_6Sn_5 and Cu_3Sn; while for the SnPb solder, the IMC layer was made of entirely Cu-Sn compound. The thickness and the shape of the IMC have great impact on the thermal cycling reliability of both types of solder joints and both factors depend on the reflow time, aging temperature and thermal cycles. Cu atoms from the Cu pad diffuse into the bulk solder and forms IMC layer and elevated temperatures increase the rate of this process. As a result the IMC grows under the elevated temperature aging, and a thicker IMC may degrade the mechanical strength of solder joint and change the failure mode due to its brittle nature. Moreover, the smoother IMC can also degrade the mechanical strength as the smoother surface has less resistance to the shear during the thermal cycling [33, 34].

The IMC thickness growth comparisons between lead-free and SnPb solder joints with various aging conditions are shown in Figure 11. In this figure, we can clearly observe that the IMC thickness tends to increase with the increase in temperature after 6 months of aging. SAC305 always had thicker IMC layer, when compared to SnPb. This phenomena, to some extent, explains the reliability trend observed in the TV7 test, where the SnPb solder joint has longer fatigue life during the thermal cycling.

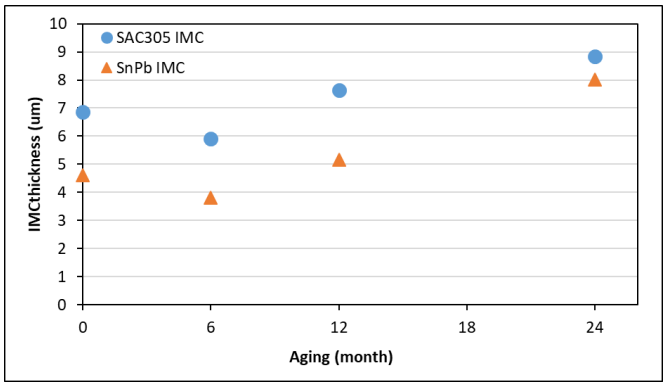

Fig. 11. IMC thickness comparisons between SAC305 and SnPb with increase of aging time

Moreover, based on a study conducted by Zhang et al. [35], the creep behavior of both lead-free and SnPb has a "crossover" where the creep rate for the lead-free solder material exceeded the SnPb after this "crossover" leading to a faster fatigue rate associated with lead-free during the thermal cycling. After that, they concluded that the microstructure evolution during aging is the "underneath" reason for the creep behavior change. For the SAC305 solder material, the coarsening of second phases is more sensitive to the aging, which is less effective in blocking the relative movement among different grains. However, the coalescence of Sn and Pb phase within the SnPb solder joints is less sensitive to the aging. This result can also explain why the SnPb outperformed lead-free after 6-month aging.

The investigations are still undergoing to try to answer the question why the reverse trend was observed in the CT1 test vehicle. The preliminary investigation results are showing that the differences in the test vehicle CTE may play a big impact on the test results, since the CT1 board is twice the thickness of the board in TV7. The higher CTE mismatch between the SnPb solder joint and PCB makes the SnPb solder joint more vulnerable to fracture, therefore, less reliability was achieved.

In the end, the differences in failure modes after thermal cycling between lead-free and SnPb solder joints for TV7 were observed and results were are shown in Figures 12 and 13. The most common failure mode across all the test vehicles was the solder crack that initiated at the corner of solder joint on the package side and propagated along the IMC layer. Other failure modes were also observed where the crack can initiate at the PCB side and propagate along the grain boundary across the bulk solder. One interesting finding from this research is that the failure mode can shift with the increasing of thermal cycles (longer dwell in the harsh applications). For a SnPb solder joint, the failure mode was consistent in thermal cycling where the cracks always propagated along the IMC on the package side (Fig.12). However, in addition to the cracks along the package side, a major crack was also observed at the bottom side of the solder joint (board side) after 5000 cycles for the SAC305 solder material (Fig. 13 lower right), which may indicate a change in the failure mode for lead-free solder joint with the increase in the number of thermal cycles.

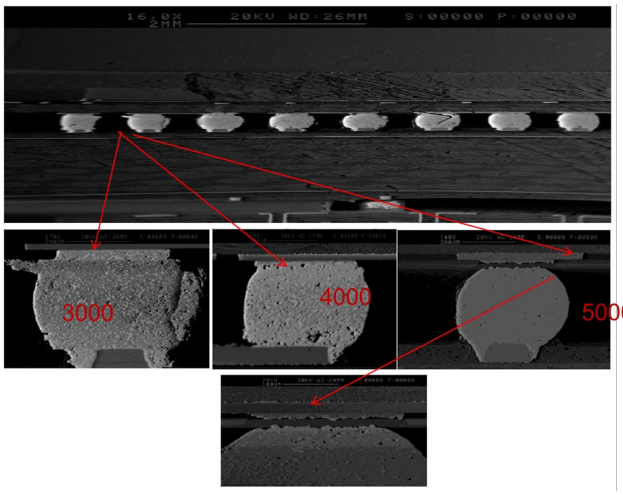

Fig. 12. Failure modes analysis for SnPb solder joints

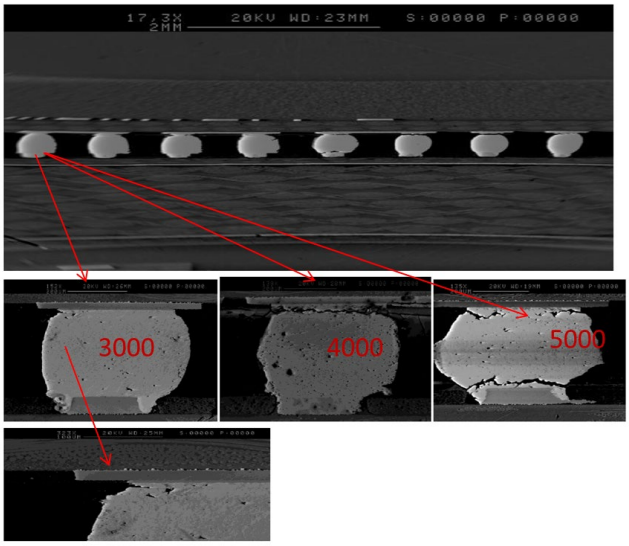

Fig. 13. Failure modes analysis for SAC305 solder joints

CONCLUSION

Two solder materials (SAC305 vs. SnPb) were compared from two different test vehicle designs in thermal cycling test. Different results were observed for each test vehicle, where SnPb demonstrated better thermal cycling reliability for different aging durations with the TV7 test vehicle, while SAC305 demonstrated better thermal cycling reliability with the CT1 test vehicle. Failure modes were analyzed after the test for TV7 test vehicle, and SnPb solder joint showed thinner IMC thickness and relatively lower creep rate after thermal cycling, which contributed to a larger fatigue life. More investigations are needed before a definitive conclusion can be drawn for the cause of the reverse trend observed in the CT1 test vehicle.

REFERENCES

[1] F. Akkara, M. Abueed, M. Rababah, C. Zhao, S. Su, J. Suhling, *et al.*, "Effect of Surface Finish and High Bi Solder Alloy on Component Reliability in Thermal Cycling," in *2018 IEEE 68th Electronic Components and Technology Conference (ECTC)*, 2018, pp. 2032-2040.

[2] Sa'd. Hamasha, F. Akkara, S. Su, H. Ali, and P. Borgesen, "Effect of Cycling Amplitude Variations on SnAgCu Solder Joint Fatigue Life," *IEEE Transactions on Components, Packaging and Manufacturing Technology,* vol. 8, pp. 1896-1904, 2018.

[3] A. Raj, T. Sanders, S. Sridhar, J. L. Evans, M. J. Bozack, W. R. Johnson, *et al.*, "Thermal Shock Reliability of Isothermally Aged Doped Lead-Free Solder with Semiparametric Estimation," *IEEE Transactions on Components, Packaging and Manufacturing Technology,* 2019.

[4] S. Su, "Reliability of Doped SnAgCu Solder Alloys with Various Surface Finishes Under Realistic Service Conditions," 2019.

[5] S. Su, F. J. Akkara, M. Abueed, M. Jian, J. Suhling, P. Lall, *et al.*, "Fatigue properties of lead-free doped solder joints," in *2018 17th IEEE Intersociety Conference on Thermal and Thermomechanical Phenomena in Electronic Systems (ITherm)*, 2018, pp. 1243-1248.

[6] M. Pecht, Y. Fukuda, and S. Rajagopal, "The impact of lead-free legislation exemptions on the electronics industry," *IEEE Transactions on Electronics Packaging Manufacturing,* vol. 27, pp. 221-232, 2004.

[7] A. Choubey, M. Osterman, and M. Pecht, "Microstructure and intermetallic formation in SnAgCu BGA components attached with SnPb solder under isothermal aging," *IEEE Transactions on Device and Materials Reliability,* vol. 8, pp. 160-167, 2008.

[8] R. Al Athamneh, M. Abueed, D. B. Hani, S. Su, J. Suhling, and P. Lall, "Effect of Aging on the Fatigue Life and Shear Strength of SAC305 Solder Joints in Actual Setting Conditions," in *2019 18th IEEE Intersociety Conference on Thermal and Thermomechanical Phenomena in Electronic Systems (ITherm)*, 2019, pp. 1146-1154.

[9] Sa'd. Hamasha, Y. Jaradat, A. Qasaimeh, M. Obaidat, and P. Borgesen, "Assessment of solder joint fatigue life under realistic service conditions," *Journal of electronic materials,* vol. 43, pp. 4472-4484, 2014.

[10] Sa'd. Hamasha, A. Qasaimeh, Y. Jaradat, and P. Borgesen, "Correlation between solder joint fatigue life and accumulated work in isothermal cycling," *IEEE Transactions on Components, Packaging and Manufacturing Technology,* vol. 5, pp. 1292-1299, 2015.

[11] Sa'd. Hamasha, S. Su, F. Akkara, A. Dawahdeh, P. Borgesen, and A. Qasaimeh, "Solder joint reliability in isothermal varying load cycling," in *2017 16th IEEE Intersociety Conference on Thermal and Thermomechanical Phenomena in Electronic Systems (ITherm)*, 2017, pp. 1331-1336.

[12] S. Su, F. J. Akkara, R. Thaper, A. Alkhazali, M. Hamasha, and Sa'd. Hamasha, "A State-of-the-Art Review of Fatigue Life Prediction Models for Solder Joint," *Journal of Electronic Packaging,* vol. 141, p. 040802, 2019.

[13] S. Su, N. Fu, F. John Akkara, and Sa'd. Hamasha, "Effect of long-term room temperature aging on the fatigue properties of SnAgCu solder joint," *Journal of Electronic Packaging,* vol. 140, 2018.

[14] S. Su, K. Hamasha, and Sa'd. Hamasha, "Effect of Surface Finish on the Shear Properties of SnAgCu-Based Solder Alloys," *IEEE Transactions on Components, Packaging and Manufacturing Technology,* vol. 9, pp. 1473-1485, 2019.

[15] S. Su, M. A. Hoque, M. M. Chowdhury, J. C. Suhling, J. L. Evans, P. Lall, *et al.*, "Mechanical Properties and Microstructural Fatigue Damage Evolution in Cyclically Loaded Lead-Free Solder Joints," in *2019 IEEE 69th Electronic Components*

and Technology Conference (ECTC), 2019, pp. 792-799.

[16] S. Su, M. Jian, F. J. Akkara, Sa'd. Hamasha, J. Suhling, and P. Lall, "Fatigue and shear properties of high reliable solder joints for harsh applications," in *SMTA International*, 2018.

[17] S. Su, M. Jian, and Sa'd. Hamasha, "Effects of Surface Finish on the Shear Fatigue of SAC-based Solder Alloys," *IEEE Transactions on Components, Packaging and Manufacturing Technology,* 2019.

[18] S. Su, M. Jian, X. Wei, F. J. Akkara, J. Suhling, P. Lall*, et al.*, "Effect of Surface Finish on the Fatigue Behavior of Bi-based Solder Joints," in *2019 18th IEEE Intersociety Conference on Thermal and Thermomechanical Phenomena in Electronic Systems (ITherm)*, 2019, pp. 1155-1159.

[19] H. Wang, J. Wang, J. Xu, V. Pham, K. Pan, S. Park*, et al.*, "Product Level Design Optimization for 2.5 D Package Pad Cratering Reliability During Drop Impact," in *2019 IEEE 69th Electronic Components and Technology Conference (ECTC)*, 2019, pp. 2343-2348.

[20] J. Wang, Y. Niu, S. Park, and A. Yatskov, "Modeling and design of 2.5 D package with mitigated warpage and enhanced thermo-mechanical reliability," in *2018 IEEE 68th Electronic Components and Technology Conference (ECTC)*, 2018, pp. 2477-2483.

[21] V. Bart, M. Gonzalez, P. Limaye, P. Ratchev, and E. Beyne, "Thermal cycling reliability of SnAgCu and SnPb solder joints: a comparison for several IC-packages."

[22] J. Zhang, S. Thirugnanasambandam, J. L. Evans, M. J. Bozack, and R. Sesek, "Impact of isothermal aging on the long-term reliability of fine-pitch ball grid array packages with different Sn-Ag-Cu solder joints," *IEEE Transactions on Components, Packaging and Manufacturing Technology,* vol. 2, pp. 1317-1328, 2012.

[23] F. Akkara, S. Su, S. Thirugnanasambandam, A. Dawahdeh, A. Qasaimeh, J. Evans*, et al.*, "Effects of long-term aging on SnAgCu solder joints reliability in mechanical cycling fatigue," in *SMTA International Conference, Rosemont, IL, Sept*, 2017, pp. 17-21.

[24] F. J. Akkara, C. Zhao, R. Athamenh, S. Su, M. Abueed, S. Hamasha*, et al.*, "Effect of Solder Sphere Alloys and Surface Finishes on the Reliability of Lead-Free Solder Joints in Accelerated Thermal Cycling," in *2018 17th IEEE Intersociety Conference on Thermal and Thermomechanical Phenomena in Electronic Systems (ITherm)*, 2018, pp. 1374-1380.

[25] F. J. Akkara, C. Zhao, S. Gordon, S. Su, M. Abueed, J. Suhling*, et al.*, "Effect of Aging on Component Reliability in Harsh Thermal Cycling," in *2019 18th IEEE Intersociety Conference on Thermal and Thermomechanical Phenomena in Electronic Systems (ITherm)*, 2019, pp. 717-723.

[26] F. J. Akkara, C. Zhao, S. Su, S. Hamasha, and J. Suhling, "Effects of mixing solder sphere alloys with bismuth-based pastes on the component reliability in harsh thermal cycling," in *SMTA International*, 2018.

[27] A. Raj, S. Sridhar, S. Gordon, J. Evans, M. Bozack, and W. Johnson, "LONG TERM ISOTHERMAL AGING OF BGA PACKAGES USING DOPED LEAD FREE SOLDER ALLOYS."

[28] A. Raj, S. Sridhar, S. Thirugnanasambandam, T. Sanders, S. Hamasha, J. Evans*, et al.*, "Comparative Study on Impact Of Various Low Creep Doped Lead Free Solder Alloys," in *SMTA International Conference Proceedings*, 2017.

[29] A. Raj, S. Thirugnanasambandam, T. Sanders, S. Sridhar, J. Evans, M. Bozack*, et al.*, "Thermal Shock Reliability Test on Multiple Doped Low Creep Lead free solder paste and Solder Ball Grid Array Packages," in *SMTA International Proceedings*, 2015.

[30] A. Raj, S. Thirugnanasambandam, T. Sanders, S. Sridhar, S. Gordon, J. Evans*, et al.*, "Proportional Hazard Model of doped low creep lead free solder paste under thermal shock," in *2016 15th IEEE Intersociety Conference on Thermal and Thermomechanical Phenomena in Electronic Systems (ITherm)*, 2016, pp. 1191-1201.

[31] J. Zhang, Z. Hai, S. Thirugnanasambandam, J. L. Evans, and M. Bozack, "Isothermal aging effects on the thermal reliability performance of lead-free solder joints," in *International Symposium on Microelectronics*, 2012, pp. 000801-000808.

[32] J. Zhang, Z. Hai, S. Thirugnanasambandam, J. L. Evans, M. J. Bozack, Y. Zhang*, et al.*, "Thermal aging effects on the thermal cycling reliability of lead-free fine pitch packages," *IEEE transactions on components, packaging and manufacturing technology,* vol. 3, pp. 1348-1357, 2013.

[33] H. Pang, K. Tan, X. Shi, and Z. Wang, "Microstructure and intermetallic growth effects on shear and fatigue strength of solder joints subjected to thermal cycling aging," *Materials Science and Engineering: A,* vol. 307, pp. 42-50, 2001.

[34] P. Tu, Y. C. Chan, and J. Lai, "Effect of intermetallic compounds on the thermal fatigue of surface mount solder joints," *IEEE Transactions on Components, Packaging, and Manufacturing Technology: Part B,* vol. 20, pp. 87-93, 1997.

[35] Y. Zhang, Z. Cai, J.C. Suhling, P. Lall, and M. J. Bozack. "The effects of aging temperature on SAC solder joint material behavior and reliability." In *2008 58th Electronic Components and Technology Conference*, pp. 99-112. IEEE, 2008.